A stamped PEDOT:PSS–silicon nanowire hybrid solar cell

Syed Abdul Moiz[1]**, Ahmed Muhammad Nahhas**[1]**, Han-Don Um**[2]**,**
Sang-Won Jee[3]**, Hyung Koun Cho**[4]**, Sang-Woo Kim**[4] **and Jung-Ho Lee**[3]

[1] Department of Electrical Engineering, College of Engineering and Islamic Architecture,
Umm Al-Qura University, Makkah, KSA
[2] Department of Bio-Nano Technology, Hanyang University, Ansan 426-791, Korea
[3] Department of Materials and Chemical Engineering, Hanyang University, Ansan,
Gyeonggi-do 426-791, Korea
[4] School of Advanced Materials Science and Engineering, Sungkyunkwan University, Suwon 440-746,
Korea

E-mail: kimsw1@skku.edu and jungho@hanyang.ac.kr

Abstract

A novel stamped hybrid solar cell was proposed using the stamping transfer technique by
stamping an active PEDOT:PSS thin layer onto the top of silicon nanowires (SiNWs).
Compared to a bulk-type counterpart that fully embeds SiNWs inside PEDOT:PSS, an
increase in the photovoltaic efficiency was observed by a factor of ∼4.6, along with
improvements in both electrical and optical responses for the stamped hybrid cell. Such
improvements for hybrid cells was due to the formation of well-connected and linearly aligned
active PEDOT:PSS channels at the top ends of the nanowires after the stamping process.
These stamped channels facilitated not only to improve the charge transport, light absorption,
but also to decrease the free carriers as well as exciton recombination losses for stamped
hybrid solar cells.

(Some figures may appear in colour only in the online journal)

1. Introduction

Recently, significant efforts have been devoted towards
optimizing the bulk hybrid structure of a solar cell that
incorporates inorganic nanowires inside polymer semiconduc-
tors [1–7]. However, some main hurdles, such as excessive
recombination of carriers, decay of excitons within an exciton
diffusion length (≤10 nm) and inefficient carrier transport
inside the polymer, cause a serious limitation to the efficiency
of hybrid solar cells [8]. Although these limitations can be
minimized by incorporating nanowires inside the optimum
thickness of the polymer close to 70 nm [9, 10], but
unfortunately such types of hybrid solar cells with nanowire
lengths lower than optimum thickness are not so practical
to utilize the offered advantages by nanowires. On the other
hand, the fabrication of a dense nanowire array, where the
inter-spacing between the nanowires is close to the exciton
diffusion length, or the synthesizing of such active polymers

which have very low exciton binding energies still remains a
challenging task for efficient hybrid solar cells [7, 11].

Here, an attempt is made to overcome these limitations by
proposing a novel idea as stamped hybrid PEDOT:PSS–SiNW
solar cells compared to the bulk hybrid solar cell,
where different bulk-type hybrid solar cells are already
well reported [1–7, 12–14]. For this purpose, a thin
layer of PEDOT:PSS was successfully transferred using
a simple stamping process onto the top of SiNWs for
photovoltaic application. As a result of the stamping
transfer, conductive channels consisting of nanowire tips
interlinked via agglomerated PEDOT:PSS were linearly
formed at the top sides of the SiNW array. To explore
the effects of stamped channels, the electrical, optical and
photovoltaic responses of a stamped PEDOT:PSS–SiNW
hybrid solar cell were investigated and compared to the
bulk-type counterparts [1–7, 12–14]. In contrast to the
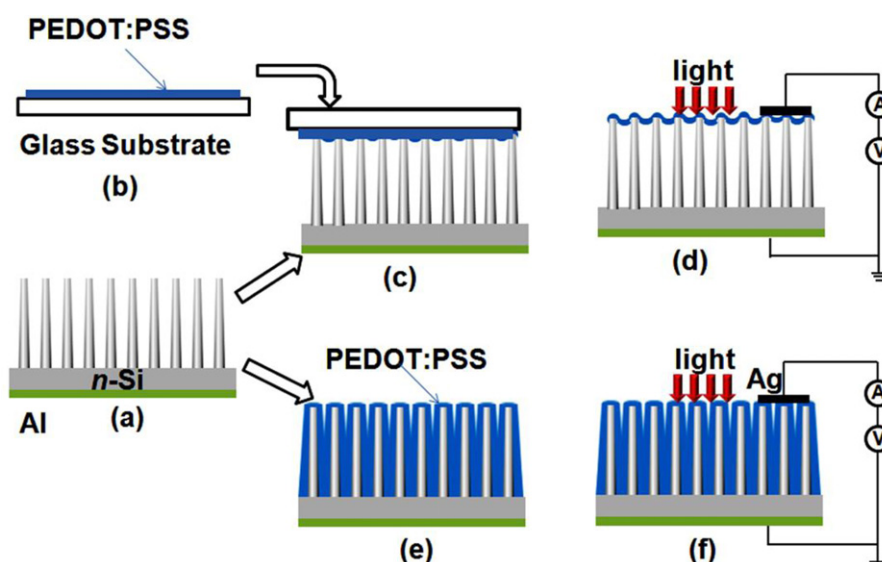bulk-type structure, a stamped hybrid cell revealed greater

Figure 1. Schematic realization of both hybrid solar cells, where (a) SiNW array with Al backsided electrode was fabricated by electroless-etching method, (b) PEDOT:PSS thin film was deposited on the surface of glass substrate by the spin-coating method for fabrication of stamped hybrid cell, (c) PEDOT:PSS was placed on top of the already prepared SiNWs during the annealing process, (d) glass substrate was detached from the top of SiNWs and then Ag electrode was deposited for electrical characterization of the stamped hybrid solar cell. (e) For fabrication of bulk hybrid solar cells, PEDOT:PSS was spin-coated on SiNW array (f) and then Ag electrode was deposited on top of the SiNW array for electrical characterization for bulk hybrid solar cells.

enhancement of the power conversion efficiency (PCE), due to the improvements of major photovoltaic parameters such as the short-circuit current, open-circuit voltage, series resistance, shunt resistance, diode ideality factor and optical reflection. These features could be understood based upon the effective exciton dynamics with the improved carrier transport and as well as efficient light absorption in the stamped PEDOT:PSS–SiNW hybrid structure. To the best of our knowledge, no such study regarding the stamped channels of a polymer as active photovoltaic material on top of SiNW arrays for hybrid solar cell applications has been reported previously.

2. Experimental procedures

The active polymer material PEDOT:PSS was purchased from Sigma-Aldrich, having 0.5 wt% aqueous solution of PEDOT with 0.8 wt% PSS, and were used in the experiment without any further purification. Figure 1 schematically summarizes the essential steps required for the fabrication for both bulk and stamped hybrid solar cells. For the fabrication of the hybrid solar cells, SiNWs were firstly grown from n-type Si wafers with resistivity 1–5 Ω cm by using the conventional electroless-etching technique; see figure 1(a). For an external electrical contact, the backsided aluminum electrode was deposited (before growing SiNWs) by using the thermal deposition method onto the highly doped very thin layer inside the back of a silicon wafer. The detailed information about the fabrication of backsided electrode and SiNWs can be found in our already reported results [15, 16]. For the fabrication of a stamped hybrid cell, a glass substrate was cleaned with detergent, distilled water, acetone and isopropyl alcohol. The ink PEDOT:PSS was spin-cast

onto a pre-cleaned glass substrate as a stamp in a glove box at 1000 rpm for 40 s, then dried for 30 min at 140 °C in a glove box (figure 1(b)). During the drying procedure, freshly spin-coated PEDOT:PSS was transferred by slightly pressing it onto the top of the SiNWs (figure 1(c)). After drying, the glass substrate was softly detached from the top of the Si nanowired substrate and left behind the linearly agglomerated stamped channels attached at the top surfaces of the SiNW array. The Ag electrode for external electrical connection was deposited at the top of the stamped PEDOT:PSS channels for a stamped hybrid solar cell (figure 1(d)). Similarly, to make the bulk-type hybrid cell (hereafter referred to as the bulk hybrid cell), the PEDOT:PSS solution was dropped on previously prepared SiNWs, left there for nearly 1 min, then spin-cast at 1000 rpm for 40 s in a glove box. Drying was done at 140 °C for 30 min in a glove box (figure 1(e)). A small patch of 100 nm thick Ag electrode was deposited on the bulk hybrid cells just like a stamped hybrid cell using a thermal evaporator under a vacuum pressure of 4×10^{-6} mbar (figure 1(f)). For characterization, the electrical current–voltage (J–V) responses of both hybrid solar cells were tested under dark and illuminated conditions using a parameter analyzer HP 4145B attached to a solar simulator (Peccel PEC-L11) at an irradiation intensity of 100 mW cm^{-2} (AM1.5 conditions).

3. Results and discussion

3.1. Morphology of bulk and stamped channels

To examine the morphology of PEDOT:PSS–SiNWs hybrid solar cells, the scanning electron microscope (SEM) characterization of both bulk and hybrid solar cells
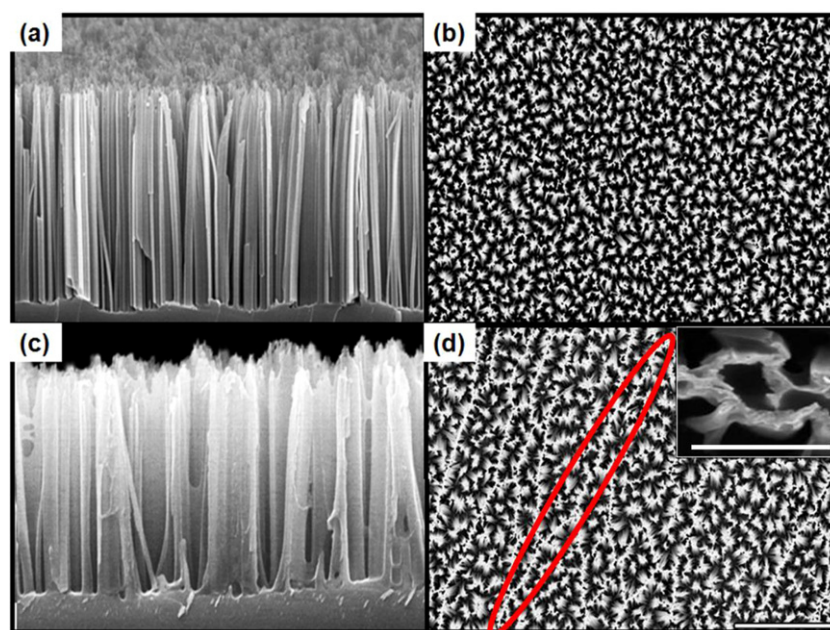
Figure 2. SEM images of (a) side view of simple SiNW arrays, (b) top view of simple SiNWs, (c) side view of SiNW embedded with PEDOT:PSS for bulk hybrid solar cell and (d) top view of SiNWs with PEDOT:PSS for the stamped hybrid cell, where the top of the SiNWs are interconnected through thin channels (a few tens of nanometers) of PEDOT:PSS, one interconnected PEDOT:PSS stamped channel is highlighted in the image. The inset of figure 1(d) shows the top view of a small portion of a stamped channel placed on the top of nanowires at 100 nm scale. All other images have scale equal to 1 μm.

were carried out and are shown in figure 2. From the side (figure 2(a)) and top view (figure 2(b)) of SiNW arrays, the resulting average length, diameter and inter-nanowire spacing of SiNWs were found to be approximately 3 μm, 200 nm and 100 nm, respectively. After spin-coating of polymer into the SiNW array for bulk hybrid solar cells, as shown in figure 2(c), the polymer were easily infiltrated into the inter-nanowire spacing and adhered at the surfaces of nanowires. Still very few voids among nanowires were observed due to the insufficient adhering of bulk polymer at the surfaces of nanowires. Such insufficient adhering of polymer was resulted from high speed spin coating and thermal annealing during the fabrication of the bulk hybrid solar cell. But, in general, most interspaces among SiNWs were occupied by the polymer as the bulk region and play a vital role to define electrical, optical and photovoltaic responses for the bulk hybrid cell, where the top view of the SiNW array for stamped hybrid solar cells is shown in figure 2(d). In contrast to the highly dispersed top ends of a conventional SiNW array (figure 2(b)), the multiple well-connected and linearly agglomerated PEDOT:PSS channels at the top of SiNW arrays were formed after removing the glass substrate for the stamped hybrid cell. These channels were well connected and provided many different paths for carrier transport to the Ag electrode at the top of the cell for electrical characterization. The typical widths of these interconnected channels were in the range of a few tens of nanometers, playing a very effective role in improving the electrical, optical and photovoltaic responses for the stamped hybrid solar cell (inset of figure 2(d)).

3.2. Dark current–voltage characterization of hybrid cells

For dark current–voltage characteristics as shown in figure 4, improved forward bias current was observed in the stamped hybrid cell compared to the bulk hybrid cell. The significant reduction of the forward current in the bulk hybrid solar cell may be due to the formation of space charge effects in the bulk PEDOT:PSS region, which has often been observed for many polymer semiconductors [17–19]. By using the standard method [20, 21], different diode parameters such as a diode ideality factor, series resistance and shunt resistance were obtained for both hybrid solar cells and are listed in table 1. The shunt resistance, arising from the leakages of current through the cell, was found approximately 9 kΩ cm^2 and 15 kΩ cm^2 for bulk and stamped hybrid solar cells, respectively. While series resistance, due to the bulk resistance itself and SiNW–polymer contact resistance, was calculated as ~147.5 and ~86.3 kΩ cm^2 for bulk and stamped hybrid solar cells, respectively. However, the ideality factor, which defines the quality interaction of polymer with nanowires, for bulk was much higher (3.5) than for stamped hybrid solar cells (2.3).

3.3. Photovoltaic characterization of hybrid cells

Similarly for photovoltaic response of both hybrid solar cells, as shown in figure 5, the open-circuit voltage, short-circuit current and fill factor were measured as 0.35 V, 3.9 mA cm^{-2} and 32% for the bulk hybrid cell, and 0.43 V, 9.38 mA cm^{-2} and 45% for the stamped hybrid cell, respectively. They also provided a striking difference in overall solar efficiency of

Table 1. Calculated electrical and photovoltaic parameters obtained from the bulk and stamped PEDOT:PSS–SiNW hybrid solar cell.

Parameters	Units	Bulk hybrid cell	Stamped hybrid cell
Diode ideality factor	n	3.5	2.3
Reverse saturation current	J_o (A cm^{-2})	13.6×10^{-6}	2.45×10^{-6}
Photogenerated voltage	J_{ph} (mA cm^{-2})	0.75	2.7
Series resistance	R_s (Ω cm^2)	147.5	86.3
Shunt resistance	R_{sh} (Ω cm^2)	9×10^3	15×10^3
Open-circuit voltage	V_{oc} (V)	0.35	0.43
Short-circuit current	J_{sh} (mA cm^{-2})	3.9	9.38
Fill factor	FF (%)	32	45
Solar efficiency	PCE (%)	0.44	1.82

0.44% for bulk and 1.82% for stamped hybrid cells. The improvement in solar efficiency for stamped hybrid solar cells was found to be a factor of ∼4.6 as compared with bulk hybrid solar cells, where improved short-circuit current contributed more than 50% of total improvement. Thus, the improvement in solar efficiency for stamped hybrid solar cells was facilitated by the stamped channels by (i) improving free carrier transport, (ii) reducing carrier recombination losses, (iii) diminishing exciton decay losses, (iv) enhancing the optical anti-reflection response and (iv) improving the open-circuit voltage.

3.3.1. Role of the stamped channels for improved carrier charge transport. The solar efficiency of hybrid solar cells is mainly defined by the nature of the carrier transport mechanism inside the polymer, whereas the heavily doped SiNW array provides a large surface area inside the polymer as electrodes for efficient charge collection. Therefore, the charge transport mechanism of the hybrid solar cell depends on the mobility of the free carriers inside the polymer. It is well accepted that the polymer thickness above 70 nm not only increases the series resistance but also lowers the intrinsic electric field between electrodes, which in turn severely degraded the mobility of carriers owing to the dispersive nature of the polymer [9, 10, 22]. Therefore the stamped channels, having thicknesses of a few tens of nm, offered lower series resistance and hence solar efficiency, due to the efficient charge mobility and hence transport mechanism, compared to the bulk hybrid solar cell (where the active bulk polymer region was greater than 100 nm) as reflected by their diode parameters in table 1.

3.3.2. Role of the stamped channels for reducing the carrier recombination losses. Similarly, solar efficiency also depends on the bulk recombination losses as well as polymer–nanowire interfacial recombination losses for hybrid solar cells. The probability of bulk recombination was expected to be high for bulk hybrid solar cells due to the high thickness dependence of the low mobility of free carriers inside the polymer [23]. On the other hand, the interfacial recombination losses are the direct function of nanowire surfaces and their interaction with the polymer for both hybrid solar cells. The quality of nanowire surfaces depends on the nature of the nanowire fabrication method.

The electroless-etching method, a common technique used for the fabrication of nanowire arrays [24], creates a series of dangling bonds at the surfaces of SiNWs. Therefore, the large surface interaction of nanowires with polymer for bulk hybrid solar cells provided a high surface trap density for recombination losses as well as leakages of current [25, 26]. On the other hand, stamped channels having very low thicknesses interacted with a small portion of the SiNW surface area compared to bulk hybrid solar cells. Therefore, compared to the bulk hybrid solar cell a relatively lower value of both bulk and interfacial recombination losses was expected due to the stamped channels for stamped hybrid solar cells and is reflected by their low value of diode ideality factor.

3.3.3. Role of the stamped channels for reducing exciton decay losses. The third major contribution of the stamped channels on the improvement of PCE for hybrid solar cells is the significant reduction of exciton decay losses. As the polymer has a very low value of exciton diffusion length such as ∼10 nm, therefore 50% of excitons have decayed after traveling just 10 nm distance inside the polymer. For that reason, most of the generated excitons had decayed in the thick PEDOT:PSS region within the exciton diffusion length, while reasonable excitons were also lost at a high interfacial trap density on SiNW surfaces, owing to the larger interfacial area between the bulk PEDOT:PSS and SiNW interfaces and led to the poor solar efficiency for the bulk hybrid cell. Subsequently, for the stamped hybrid cell excitons were generated in the thin stamped channels, while a relatively large number of generated excitons survived inside the polymer due to nanometer scale thin stamped channels, while a relatively small portion of excitons were also lost at lower interfacial trap density on the SiNW surfaces compared to the bulk hybrid solar cell. Therefore, the very thin stamped channels also significantly improved the exciton decay losses for efficient stamped hybrid solar cells.

3.3.4. Role of the stamped channels for improving optical reflection. For measuring the improvement in anti-reflection response, the total optical reflection spectra for both hybrid solar cells were measured using a Varian Cary 5000 UV/vis/NIR spectrophotometer with an integrating sphere (Labsphere) in a wavelength range of 300–1100 nm, and are shown in figure 3. From the total optical reflection spectra
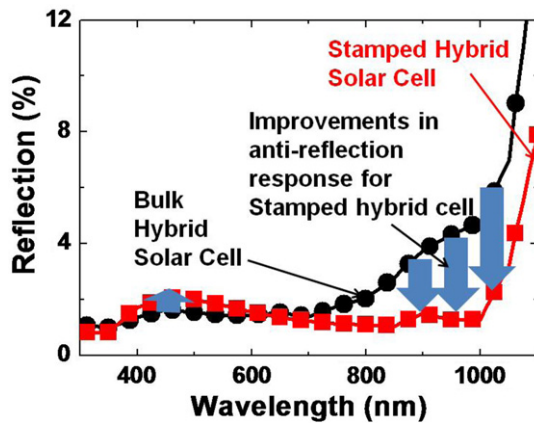
Figure 3. Optical reflectance spectra for the stamped and bulk hybrid solar cell. The bulk hybrid cell shows slightly enhanced anti-reflection for the wavelength range of 300–700 nm, but the anti-reflection above 700 nm is very significantly enhanced for the stamped hybrid solar cell compared with the bulk hybrid cell.

for both hybrid cells, the bulk hybrid cell showed slightly enhanced anti-reflection as compared to the stamped hybrid cell in the wavelength range of 400–600 nm, which covers only a small fraction of the total solar spectrum. Generally, PEDOT:PSS has a higher bandgap (∼1.6 eV) [27] and lower refractive index (∼1.53) [28] compared to Si. Therefore the small improvement in the anti-reflection response in the given wavelength range could be attributed to the higher optical absorption by the larger bulk quantity of polymer compared to the thin stamped polymer channels for the bulk hybrid solar cell. However, stamped channels showed an excellent anti-reflection response for the wavelength range 600–1100 nm, which accounts for greater than 50% of the photon flux of the entire solar spectrum [29]. At a wavelength spectrum above ∼700 nm, greater than the bandgap absorption edges of bulk PEDOT:PSS for optical absorption, the bulk quantity of PEDOT:PSS did not play any significant role in optical absorption. Therefore, the stamped channels of the hybrid cell offered less resistance to the light propagation for the given wavelength range, because most of the surface area along the SiNWs was occupied by air. Such lesser hindrances also enhanced the optical absorption by enlarging the optical path inside the SiNW array due to multiple optical scattering among nanowires for stamped hybrid solar cells. On the other hand, for the same wavelength range, highly reflective PEDOT:PSS (compared to air) occupied most of the surface area along the SiNWs, so therefore very high reflection was observed for bulk hybrid cells. Therefore, the stamped channels for the hybrid solar cell significantly improve the overall optical anti-reflection response compared to the bulk hybrid solar cell.

3.3.5. Role of the stamped channels for improving open-circuit voltage. Most factors discussed above regarding the improvements of solar efficiency, facilitated by the stamped channels, are directly associated with the short-circuit current
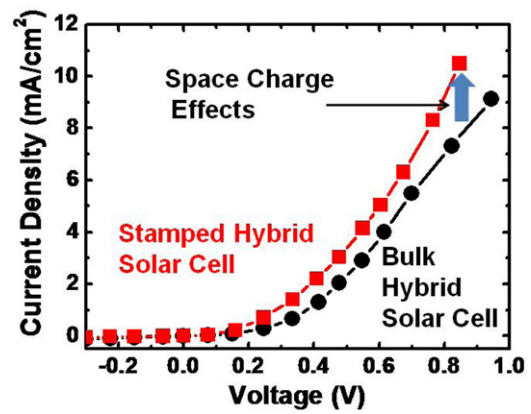

Figure 4. Dark current–voltage characteristics for both the stamped and bulk hybrid cells. It can clearly be observed that the bulk hybrid cell follows the space–charge-limited current at higher forward biasing.
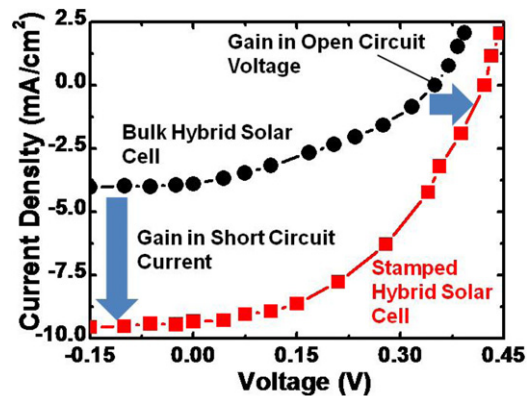

Figure 5. Illuminated current–voltage characteristics for both cells under AM1.5G illumination for photovoltaic measurement, where the stamped hybrid solar cell shows significant improvement in short-circuit current and open-circuit voltage.

of the stamped solar cells. However, low series resistance and high shunt resistance are also responsible for improving the fill factor for stamped channels compared to the bulk hybrid solar cell. But, regardless of the similarity of the materials and low diode ideality factor, an improvement in the open-circuit voltage (V_{oc}) for the stamped hybrid cell can be justified by approximating the ideal solar cell equation for V_{oc} such as [30]

$$V_{oc} \approx \frac{nkT}{q} \ln\left[\frac{J_{ph}(V_{oc})}{J_o} + 1\right] \approx \frac{nkT}{q} \ln\left[\frac{J_{ph}(V_{oc})}{J_o}\right], \quad (1)$$

where k is the Boltzmann constant, T is ambient temperature, q is electrical charge, n is diode ideality factor and J_o is reverse saturation current, while the photogenerated voltages ($J_{ph}(V_{oc})$) are calculated at $V = V_{oc}$ from dark J–V responses for both hybrid cells (table 1). By using the logarithm of the ratio of $J_{ph}(V_{oc})/J_o$, a higher value of V_{oc} is obtained for the stamped hybrid cell, even with a low diode ideality factor. Hence, the enhancement of V_{oc} is the direct outcome of both the increment in $J_{ph}(V_{oc})$ and a decrement in J_o, stem from the low series resistance of channels and improvement in the

leakage current at polymer–nanowire interfaces for stamped hybrid solar cells.

4. Conclusions

In conclusion, we successfully demonstrated the fabrication of a hybrid solar cell by stamping the active PEDOT:PSS layer onto the top of SiNWs for efficient photovoltaic application. In contrast to the bulk PEDOT:PSS hybrid cell, electrical, optical and photovoltaic responses were significantly enhanced due to efficient charge transport, better light absorption and considerable reduction of free carrier recombination as well as reduction in exciton decay losses for the stamped hybrid solar cell. As in this study, parameters for the stamped hybrid solar cell are not fully optimized; therefore, there is considerable room available for further efficiency improvement such as (i) selection of suitable polymer material, (ii) optimal thickness of polymer layer, (iii) optimal length and diameter of nanowire array and (iv) improving top contact series resistance by using a metal grid as an electrode. But overall our demonstration for the stamped PEDOT:PSS–SiNW hybrid solar cell might have important implications for the fabrication of a highly efficient polymer–nanowire hybrid solar cell for future applications.

Acknowledgments

References

[1] Huynh W U, Dittmer J J and Alivisatos A P 2002 Hybrid nanorod–polymer solar cells *Science* **295** 2425–7

[2] Kim C H, Cha S H, Kim S C, Song M, Lee J, Shin W S, Moon S-J, Bahng J H, Kotov N A and Jin S H 2011 Silver nanowire embedded in P3HT:PCBM for high-efficiency hybrid photovoltaic device applications *ACS Nano* **5** 3319–25

[3] Zhang F, Sun B, Song T, Zhu X and Lee S 2011 Air stable, efficient hybrid photovoltaic devices based on poly(3-hexylthiophene) and silicon nanostructures *Chem. Mater.* **23** 2084–90

[4] Briseno A L, Holcombe T W, Boukai A I, Garnett E C, Shelton S W, Frechet J J M and Yang P 2010 Oligo- and polythiophene/ZnO hybrid nanowire solar cells *Nano Lett.* **10** 334–40

[5] Novotny C J, Yu E T and Yu P K L 2008 InP nanowire/polymer hybrid photodiode *Nano Lett.* **8** 775–9

[6] Shiu S C, Chao J J, Hung S C, Yeh C L and Lin C F 2010 Morphology dependence of silicon nanowire/poly(3,4-ethylenedioxythiophene): poly(styrenesulfonate) heterojunction solar cells *Chem. Mater.* **22** 3108–13

[7] Ren S, Zhao N, Crawford S C, Tambe M, Bulovic V and Gradecak S 2011 Heterojunction photovoltaics using GaAs nanowires and conjugated polymers *Nano Lett.* **11** 408–13

[8] Bredas J L, Beljonne D, Coropceanu V and Cornil J 2004 Charge-transfer and energy-transfer processes in π-conjugated oligomers and polymers: a molecular picture *Chem. Rev.* **104** 4971–5003

[9] Friedel B, Keivanidis P E, Brenner T J K, Abrusci A, McNeill C R, Friend R H and Greenham N C 2009 Effects of layer thickness and annealing of PEDOT:PSS layers in organic photodetectors *Macromolecules* **42** 6741–7

[10] Brenner T J K, Hwang I, Greenham N C and McNeill C R 2010 Device physics of inverted all-polymer solar cells *J. Appl. Phys.* **107** 11450

[11] Gelinas S, Labrosse O P, Brosseau C N, Seifried S A, McNeill C R, Kirov K R, Howard I A, Leonelli R, Friend R H and Silva C 2011 The binding energy of charge-transfer excitons localized at polymeric semiconductor heterojunctions *J. Phys. Chem. C* **115** 7114–9

[12] Liu J, Wang S, Bian Z, Shan M and Huang C 2009 Organic/inorganic hybrid solar cells with vertically oriented ZnO nanowires *Appl. Phys. Lett.* **94** 173107

[13] Bi D, Wu F, Yue W, Guo Y, Shen W, Peng R, Wu H, Wang X and Wang M 2010 Device performance correlated with structural properties of vertically aligned nanorod arrays in polymer/ZnO solar cells *J. Phys. Chem. C* **114** 13846–52

[14] Woo S, Lee S S, Han Y, Lyu H, Kim K, Kim H and Kim Y 2010 Hybrid solar cells based on bulk heterojunction films of conjugated polymers and single crystalline Si nanowires *J. Nanoelectron. Optoelectron.* **5** 139–42

[15] Moiz S A, Jee S W, Um H D and Lee J-H 2010 Electrical characterization of metal–silicon microwire interface using conductive atomic force microscope *Japan. J. Appl. Phys.* **49** 045003

[16] Um H D, Jung J Y, Seo H S, Park K T, Jee S W, Moiz S A and Lee J-H 2010 Silicon nanowire array solar cell prepared by metal-induced electroless etching with a novel processing technology *Japan. J. Appl. Phys.* **49** 04DN02

[17] Mihailetchi V D, Wildeman J and Blom P W M 2005 Space-charge limited photocurrent *Phys. Rev. Lett.* **94** 126602

[18] Moiz S A, Ahmed M M, Karimov Kh S, Rehman F and Lee J-H 2009 Space charge limited current–voltage characteristics of organic semiconductor diode fabricated at various gravity conditions *Synth. Met.* **159** 1336–9

[19] Moiz S A, Ahmed M M, Karimov Kh S and Mehmood M 2007 Temperature-dependent current–voltage characteristics of poly-N-epoxypropylcarbazole complex *Thin Solid Films* **516** 72–7

[20] Lin M Y, Lee C Y, Shiu S C, Wang I J, Sun J Y, Wu W H, Lin Y H, Huang J S and Lin C-F 2010 Sol–gel processed CuOx thin film as an anode interlayer for inverted polymer solar cells *Org. Electron.* **11** 1828–34

[21] Karimov Kh S, Ahmed M M, Moiz S A and Fedorov M I 2005 Temperature-dependent properties of organic-on-inorganic Ag/p–CuPc/n–GaAs/Ag photoelectric cell *Sol. Energy Mater. Sol. Cells* **87** 61–75

[22] Kline R J and McGehee M D 2006 Morphology and charge transport in conjugated polymers *J. Macromol. Sci. C Polym. Rev.* **46** 27–45

[23] Koster L J A, Smits E C P, Mihailetchi V D and Blom P W M 2005 Device model for the operation of polymer/fullerene bulk heterojunction solar cells *Phys. Rev. B* **72** 085205

[24] Kato Y and Adachi S 2011 Synthesis of Si nanowire arrays in AgO/HF solution and their optical and wettability properties *J. Electrochem. Soc.* **158** K157–63

[25] Schmidt V, Wittemann J V, Senz S and Gosele U 2009 Silicon nanowires: a review on aspects of their growth and their electrical properties *Adv. Mater.* **21** 2681–702

[26] Yuan G, Aruda K, Zhou S, Levine A, Xie J and Wang D 2011 Understanding the origin of the low performance of chemically grown silicon nanowires for solar energy conversion *Angew. Chem. Int. Edn* **50** 2334–8

[27] Greczynskia G, Kuglerb Th, Keila M, Osikowicza W, Fahlmanc M and Salanecka W R 2001 Photoelectron spectroscopy of thin films of PEDOT–PSS conjugated polymer blend: a mini-review and some new results *J. Electron Spectrosc. Relat. Phenom.* **121** 1–17

[28] Pettersson L A A, Ghosh S and Inganas O 2002 Optical anisotropy in thin films of poly(3,4-ethylenedioxythiophene)–poly(4-styrenesulfonate) *Org. Electron.* **3** 143–8

[29] Rand B P, Xue J, Yang F and Forrest S R 2005 Organic solar cells with sensitivity extending into the near infrared *Appl. Phys. Lett.* **87** 233508

[30] Sze S M 1981 *Physics of Semiconductor Devices* (New York: Wiley)